Thin Solid Films 612 (2016) 317–321

Contents lists available at ScienceDirect

Thin Solid Films

journal homepage: www.elsevier.com/locate/tsf

Ultra-thin planar tunnel junctions grown on Nb thin films by atomic layer deposition

Han Zhao *, Omar Mehio, Wan Kyu Park, Laura H. Greene [1]

Department of Physics & Materials Research Laboratory, University of Illinois at Urban-Champaign, Urbana, IL 61801, USA

ARTICLE INFO

Article history:
Received 12 December 2015
Received in revised form 20 May 2016
Accepted 7 June 2016
Available online 8 June 2016

Keywords:
Tunnel junction
Ultra-thin barrier
Atomic layer deposition
Electronic density of states

ABSTRACT

Atomic layer deposition (ALD) is used to grow ultra-thin and low-defect Al_2O_3 tunnel junction barriers on sputter-deposited Nb thin films. Junctions of sizes on the order of $100 \times 100\ \mu m^2$ and barrier thicknesses of 4.4 to 11 Å exhibit over 90% reproducibility. The conductance characteristics at low temperature show the clear density of states signature of superconducting Nb. The junction resistance times area product increases exponentially with barrier thickness, further supporting the high quality of the junctions, in which single-step elastic tunneling predominates. The background conductance at low temperature could not be fit with the Brinkman-Dynes-Rowell model, indicating the barriers are not likely to act as a trapezoidal potential. Our work shows that ALD is an effective method in preparing planar tunnel junctions with ultra-thin barriers.

1. Introduction

Electron tunneling spectroscopy has been used extensively to study the spectroscopic properties of superconducting materials, particularly their superconducting density of states [1,2]. Although scanning tunneling spectroscopy (STS) [3] exhibits unprecedented spatial resolution, planar tunneling spectroscopy is far more robust to vibration, and it is much more amenable to measurements as a function of temperature and applied fields.

The tunnel barrier is crucial to the overall performance of the tunnel junction and various barrier formation methods have been reported, including the direct growth of a thin layer of insulating material [4], thermal [5] and plasma oxidation [6] of either a thin metal layer or the surface of the bottom electrode [7]. However, each of these traditional methods has its own drawbacks. Sputter/evaporator-growth of an insulating compound is non-trivial and the deposited thin layer may not uniformly adhere to the sample surface. Thermal and plasma oxidation are not completely controllable processes: tunnel barriers achieved via oxidation generally are not uniform locally, which may allow current to leak through the barrier.

Aluminum oxide (Al_2O_3) grown by atomic layer deposition (ALD) has been recently used for the growth of planar tunnel junctions and Josephson junctions of areal size of a few square microns [8,9]. Microfabrication methods such as photolithography and e-beam lithography are required to make such small devices. For samples with rough surfaces, large-area junctions may not be uniform if the barrier is too thin. However, such junctions can still be uniform if the coating of the barrier layer is conformal to the sample surface as demonstrated for ALD. We have grown such junctions of sizes on the order of $100 \times 100\ \mu m^2$ on Nb thin films and found that they are quite robust.

ALD is a chemical vapor growth technique that uses self-limited surface reactions to grow films in an atomic layer-by-layer fashion, yielding precise sub-nanometer thickness control [10]. It is also used for conformal film growth [11,12]. Because of its precise control, ALD presents some advantages over other deposition techniques such as sputtering, evaporation and molecular beam epitaxy. Due to its broad application prospects, ALD growth of Al_2O_3 has been developed, based on the chemical vapor reaction [12]:

$$2Al(CH_3)_3 + 3H_2O \rightarrow Al_2O_3 + 6CH_4 \quad (1)$$

In general, this reaction is done via the following two steps in sequence:

$$AlOH^* + Al(CH_3)_3 \rightarrow AlOAl(CH_3)_2{}^* + CH_4 \quad (2)$$

$$AlCH_3{}^* + H_2O \rightarrow AlOH^* + CH_4 \quad (3)$$

During the reactive growth, alternating gaseous precursors of trimethylaluminum (TMA) and H_2O are brought to the sample surface by an N_2 gas carrier of ultra-high purity (99.999%). Pulses are separated by N_2 gas flushes to ensure different precursors do not interact in gaseous state. For Nb thin films, an H_2O pulse is applied at the beginning as the hydroxyl groups help the bonding to the sample surface. This is

* Corresponding author.
E-mail address: hanzhao2@illinois.edu (H. Zhao).
[1] Present address: National High Magnetic Field Laboratory and Department of Physics, Florida State University, Tallahassee, FL 32310, USA.

http://dx.doi.org/10.1016/j.tsf.2016.06.015
0040-6090/

followed by an N_2 purge to remove excessive H_2O molecules. The same process is then applied to TMA, facilitating the Al-methyl group to be absorbed and bonded to the hydroxyl group. This sequential exposure to H_2O and TMA constitutes a typical ALD cycle [12] and is repeated to achieve the desired film thickness.

2. Experimental details

Al_2O_3 ALD films are grown using H_2O (Optima grade) and TMA (semiconductor grade). Substrates are c-cut Al_2O_3 sapphire (0.495 in. long × 0.295 in. wide × 0.02 in. thick). The Nb sputter target is 99.95% pure and the thermally evaporated counter electrode is grown from 99.9% pure Ag metal.

The junction structure is shown in Fig. 1(a), and similar to that used in other experiments [13]. Nb films are sputter deposited at 480 °C onto sapphire substrates at a base pressure of $3–4 \times 10^{-9}$ Torr. Sputtering is done in 4 mTorr of research purity Ar (99.9999%). The 600 Å-thick Nb films used for tunnel junctions reported here exhibit $T_c = 9.0$ K, close to that of bulk Nb. These Nb films are transported to the ALD system in an N_2-filled sealed container within 10 min of removal from the sputter chamber. The Al_2O_3 tunnel barriers are grown in a commercial ALD system (Cambridge Nanotech) using the parameters shown in Table 1, with the chamber temperature set to 80 °C, and the N_2 gas flow set to 10 sccm. The deposition rate is 1.1 Å/cycle, calibrated using interferometry on a 900-cycle Al_2O_3 film. Tunnel junctions of barrier thickness from 4.4 Å (4 cycles) to 11 Å (10 cycles) are prepared. After removal from the ALD system, the junction area is defined by painting the Nb film edges with a diluted Duco cement solution [7,13] and within a few minutes, the sample is transported to a thermal evaporator for the deposition of the Ag counter electrode (2500 Å) through a shadow mask. Fig. 1(b) is an optical image of two junctions showing their uniformity.

The Nb thin films are characterized by resistivity *vs.* temperature measurements using the standard four-probe method, from which the room-temperature resistivity, residual resistivity ratio (RRR), and T_c are obtained. The room-temperature resistivity of the Nb film is 16.1 μΩ cm, the RRR ~35, and T_c ~9.0 K. Differential conductance of the tunnel junctions is measured using the standard four-probe lock-in technique.

3. Results

Fig. 2 shows the topography as measured by atomic force microscopy (AFM). The roughness map of the junction is shown in Fig. 2(a). Fig. 2(b)–(d) show the AFM image of a bare substrate, an as-grown Nb film, and an ALD Al_2O_3 coated Nb film, respectively. These data, taken with the same cantilever and on the same day, show a similar peak-to-peak roughness of less than 10 Å.

Table 1
H_2O and TMA precursor settings for ALD growth of Al_2O_3.

Gas	Pulse(s)	Purge (s)	Precursor heater temperature (°C)
H_2O	0.03	65	150
TMA	0.03	65	75

More than one hundred junctions have been made and 90% of them show the density of states signature of superconducting Nb at low temperature (Fig. 3). For reference, junctions were also prepared on an as-grown Nb film, without the Al_2O_3 barrier; none of them showed tunneling behavior. The junction R × A at room temperature for junctions with 4, 6, 8, and 10 cycles of Al_2O_3 are plotted in Fig. 4, showing an exponential dependence over a broad thickness range (see Section 4 for discussion).

The junctions are characterized as shown in Fig. 5. All these data are taken on the same junction with 6-cycle Al_2O_3, but all the junctions of different barrier thicknesses exhibit similar results. In Fig. 5(a) and (b), the experimental data are fit using the Blonder-Tinkham-Klabwijk (BTK) model [14] with the dimensionless barrier strength Z, superconducting energy gap size Δ, and the quasiparticle lifetime broadening factor Γ. The tunnel current across the junction is given by the following equation [14]:

$$I_{NS}(V) = 2A \cdot N(0) e v_F \int_{-\infty}^{\infty} [f(E-eV) - f(E)][1 + A(E) - B(E)]dE, \quad (4)$$

where $A(E)$ corresponds to the probability for Andreev reflection and $B(E)$ is the probability for normal reflection. The barrier at the interface is modeled as a delta function $V(x) = H\delta(x)$, with the barrier strength defined by a dimensionless parameter $Z = \frac{mH}{\hbar^2 k_F} = H/\hbar v_F$. The Z parameter enters explicitly in the expressions for the probability of Andreev and normal reflection. In Fig. 5(c) and (d), normalized conductance at different temperatures and magnetic fields are fit yielding a large Z (=4) and small Γ/Δ (<1%). A fit using the Bardeen-Cooper-Schrieffer (BCS) gap equation to the extracted superconducting energy gaps at different temperatures is provided in Fig. 5(c), showing the well-known weak coupling behavior.

The background conductance of junctions with 8 and 10 cycles of Al_2O_3 is fit to the Brinkman-Dynes-Rowell (BDR) model [15] to determine the barrier shape. Due to their small resistances (<10 Ω), junctions with 4 and 6 cycles of Al_2O_3 could not be biased to voltages large enough to properly measure the background conductance. As will be discussed in Section 4, the barrier shape differs from that of traditional, thicker barriers.

We note these junctions were found to be robust over time: No significant changes to the conductance characteristics were observed after

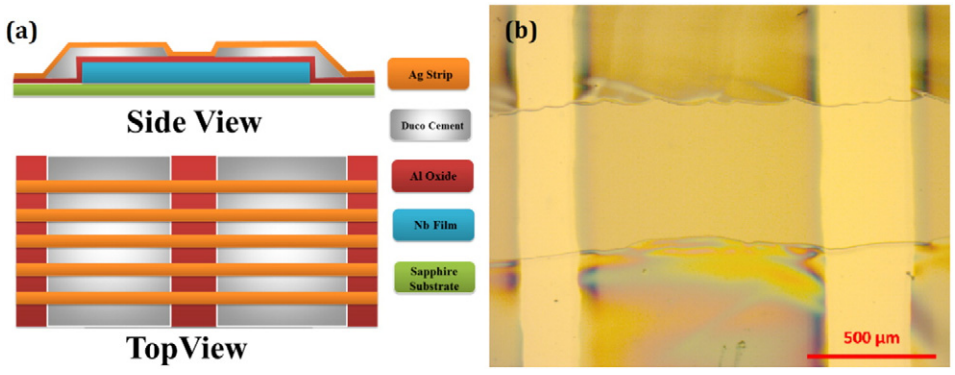

Fig. 1. (a) Illustration of junction configuration, from the bottom to top (side view): sapphire substrates (green), Nb film (bottom electrode, blue), Al_2O_3 (tunnel barrier, red), Duco cement defining junctions (grey), and Ag strip (top electrode, gold); (b) Optical image showing uniform junction areas.

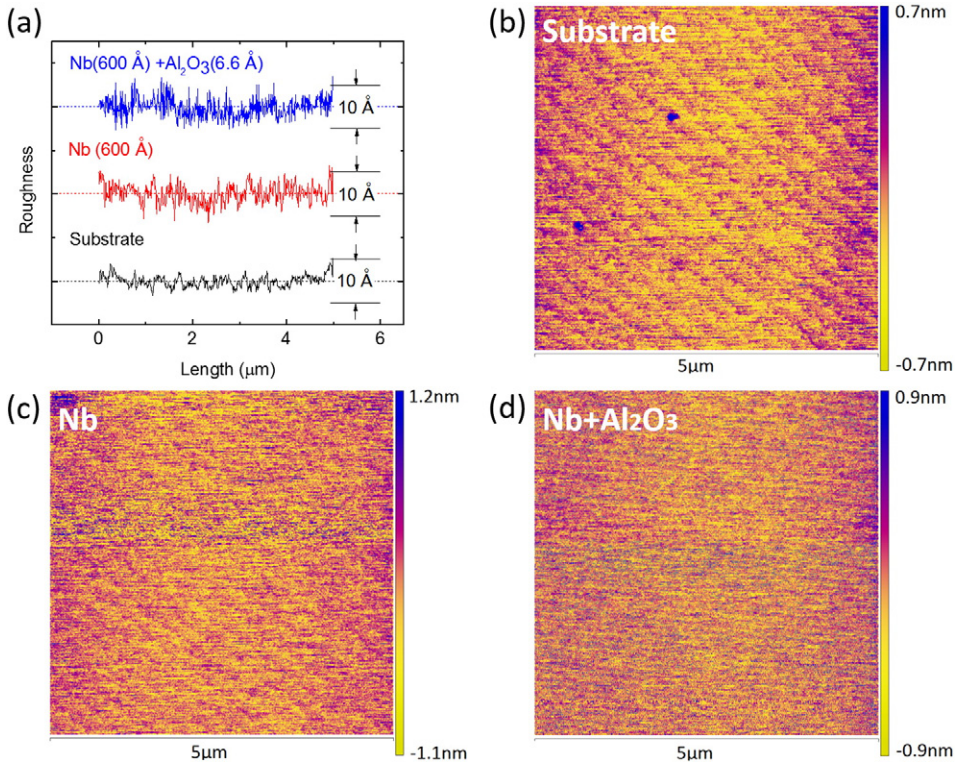

Fig. 2. AFM results. (a) Cross sectional topographic roughness; (b) Image of sapphire substrate; (c) Image of an Nb thin film; (d) Image of an Nb thin film coated with 6.6 Å of Al_2O_3. The peak-to-peak roughness of the substrate is less than 4 Å, and that of the Nb and the coated Nb is each less than 10 Å.

junctions remained at room temperature in an N_2 atmosphere for 3 weeks.

4. Discussion

The high quality of our junctions is demonstrated by the high Z value (>4) and small quasiparticle lifetime broadening factor ($\Gamma/\Delta < 1\%$) obtained from our BTK fits. A definitive test of uniformity of barrier thickness is shown in Fig. 4, where the junction R × A product *vs* barrier thickness is plotted, showing an exponential dependence over a wide thickness range. We do note that for the 4 and 6 cycle barriers, the slope is slightly smaller than in the thicker range, which we attribute to the difference in how the Al_2O_3 layer is coated in the initial cycles from the rest and thus its varying degrees of impact on the overall junction tunneling characteristics.

We find our ultra-thin barriers do not exhibit the standard trapezoidal shape in thickness *vs.* potential, typically observed in good quality planar tunnel junctions [16]. This is evidenced by our fit to the Brinkman-Dynes-Rowell (BDR) model [15], where the background conductance is fit to a parabola and the fitting parameters reveal the

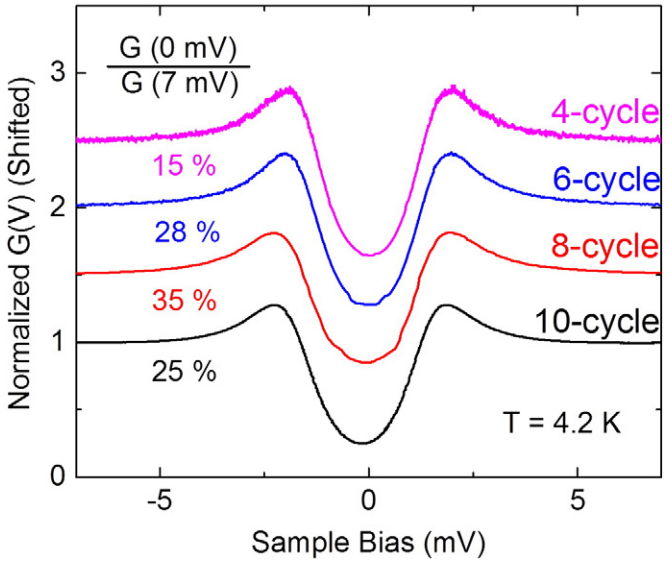

Fig. 3. Junction conductance normalized to that at 7 mV as a function of bias voltage for junctions of different tunnel barrier thicknesses (listed as number of ALD cycles) taken at 4.2 K are shown. Each of the top three curves is shifted vertically from the one below by 0.5 for clarity. The zero bias conductance value as a percentage of the background conductance is listed for each junction.

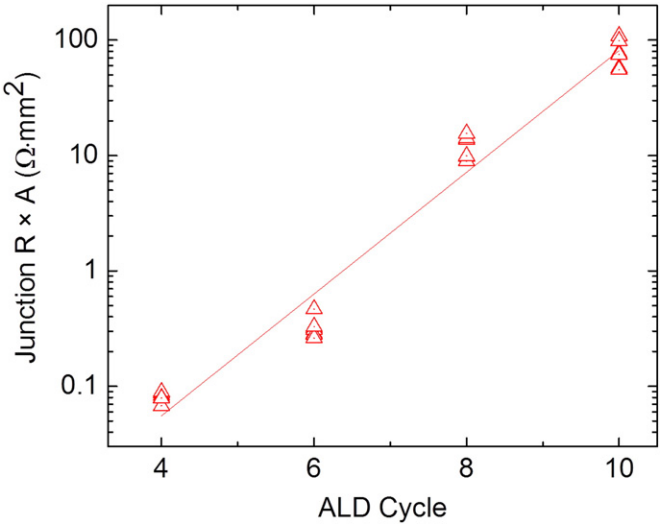

Fig. 4. The junction R × A increases approximately exponentially with barrier thickness, indicating the uniformity of the tunnel barriers, and that the predominant transport across the junction is single-step elastic tunneling.

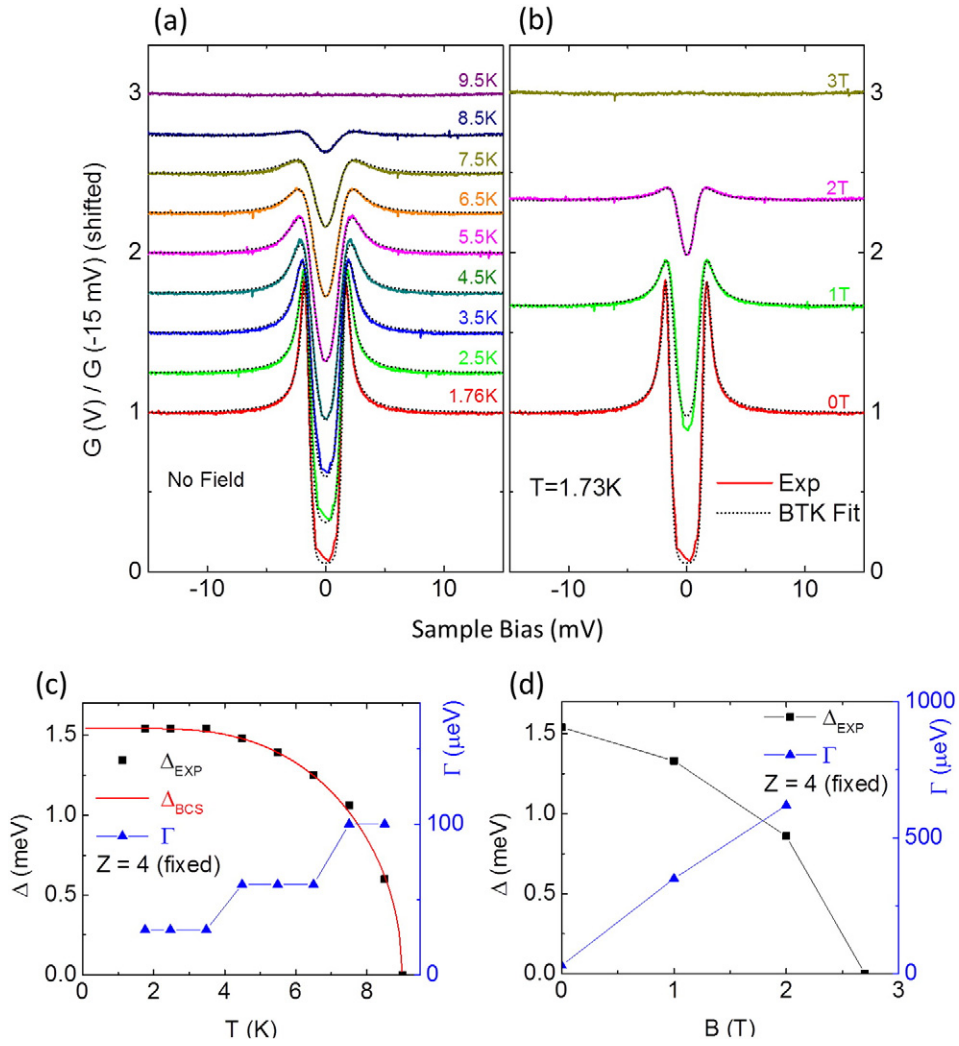

Fig. 5. Junction characterization using the BTK model on a junction with 6-cycle Al_2O_3 as a function of temperature and magnetic field applied perpendicular to the junction area. Normalized conductance data (lines) at different temperatures (a) and applied fields (b) and their BTK theory fit (points). Curves are shifted vertically for clarity. The corresponding BTK fitting parameters (Δ, Γ, and Z) as a function of temperature and field are plotted in (c) and (d), respectively. A large and constant value of $Z = 4$ is found. Because Γ is related to the quasiparticle lifetime broadening, it increases with the temperature and magnetic field, as expected. The BCS theory fit to the extracted energy gaps at different temperatures is shown as the solid red line in (c).

median height and asymmetry in the potential barrier shape. Fig. 6 presents the background conductance for junction barriers grown with 8 and 10 cycles of Al_2O_3. For these ultra-thin tunnel junctions, the fits in the low-bias range up to 100 mV (Fig. 6(b) and (c)) look good but with a barrier height of 10–20 mV for 10-cycle Al_2O_3 tunnel junctions and ~3 mV for 8-cycle, which are unrealistically small for the barrier height considering that the junctions exhibit high quality tunneling features for superconducting Nb (Fig. 5). We also stress that a BDR fit only at low bias would not be a true measure of barrier shape, as this model is devised for the analysis of the background conductance, hence, data taken over a broad bias range. However, our attempts to fit over wider biases, shown in Fig. 6(d), give even smaller values for the barrier height. Technically, this is due to the unusually rapid increase of the conductance with bias voltage. We speculate that these high-quality barriers may not be trapezoidal in shape and reasons for this are under study.

5. Conclusions

ALD is used to prepare ultra-thin Al_2O_3 tunnel barriers for junctions of sizes on the order of $100 \times 100\ \mu m^2$ and thicknesses on the order of single angstroms. The observed clear signatures for the superconducting DOS of Nb and the reproducibility greater than 90% indicate the high quality of the junctions. The junction resistance × area (R × A) product generally increases exponentially with barrier thickness, indicating that the tunnel barriers are uniform and single-step elastic tunneling predominates.

Compared with traditional thin film growth techniques, such as sputtering and thermal evaporation, ALD provides precise control of the barrier thickness and uniformity over a large area. We believe this technique to grow ultra-thin and robust planar tunnel junctions will have broad applications in microelectronics and in the study of the electronic structure in novel materials that have proven challenging to grow planar tunnel junctions, such as the high-temperature superconductors.

Acknowledgements

The authors thank Yizhi Fang, Fubo Rao, Tao Shang, Lunan Sun, and Jiang Wang for helpful discussion and advice. This work is supported by the Center for Emergent Superconductivity, an Energy Frontier Research Center funded by the U.S. Department of Energy, Office of Science, Office of Basic Energy Sciences under Award Number DE-AC0298CH1088. WKP is supported by U.S. NSF DMR under Award No. 12-06766.

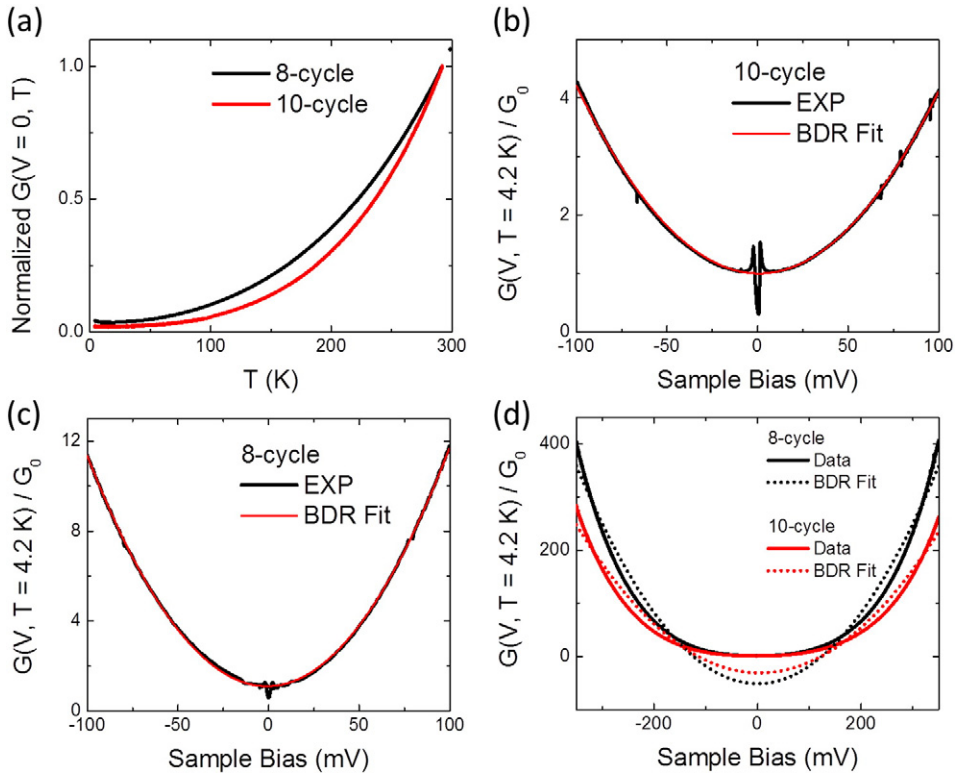

Fig. 6. Background conductance for junctions grown with 10 and 8 cycles of Al_2O_3. (a) The zero-bias conductance normalized to that at room temperature shows an unusually large decrease: 40 and 20 times for the 10 and 8 cycle thickness barriers, respectively, when the temperature is lowered from room to 4.2 K. (b) and (c) Background conductance for 10-cycle and 8-cycle Al_2O_3 tunnel junction at lower bias could be fit to the BDR model, but extracted barrier shapes are not consistent with our data. (d) Background conductance up to ±350 mV and best fit to the BDR model.

References

[1] W.L. McMillan, J.M. Rowell, in: R.D. Parks, Marshall-Dekker (Eds.),Superconductivity, 1 1969, p. 561 New York.
[2] E.L. Wolf, Principles of Electron Tunneling Spectroscopy, International Series of Monographs on Physics, Oxford University Press, New York, 1985.
[3] J.W. Harold, Arie van Houselt Zandvliet, Scanning tunneling spectroscopy, Annu. Rev. Anal. Chem. 2 (2009) 37–55.
[4] L.H. Greene, M. Covington, M. Aprili, E. Badica, D.E. Pugel, Observation of broken time-reversal symmetry with Andreev bound state tunneling spectroscopy, Physica B 280 (2000) 159–164.
[5] J.C. Fisher, I. Giaever, Tunneling through thin insulating layers, J. Appl. Phys. 32 (1961) 172–177.
[6] J.L. Miles, P.H. Smith, The formation of metal oxide films using gaseous and solid electrolytes, J. Electrochem. Soc. 110 (1963) 1240–1245.
[7] K. Chen, W. Dai, C.G. Zhuang, Q. Li, S. Carabello, J.G. Lambert, J.T. Mlack, R.C. Ramos, X.X. Xi, Momentum-dependent multiple gaps in magnesium diboride probed by electron tunnelling spectroscopy, Nat. Commun. 3 (2012) 619.
[8] T. Dirks, T.L. Hughes, S. Lal, B. Uchoa, Y.-F. Chen, C. Chialvo, P.M. Goldbart, N. Mason, Transport through Andreev bound states in a graphene quantum dot, Nat. Phys. 7 (2011) 386–390.
[9] A.J. Elliot, G. Malek, L. Wille, R. Lu, S. Han, J.Z. Wu, J. Talvacchio, R.M. Lewis, Probing the nucleation of Al_2O_3 in atomic layer deposition on aluminum for ultrathin tunneling barriers in Josephson junctions, Appl. Supercond. 23 (2013) 1100705.
[10] N. Pinna, M. Knez, Atomic Layer Deposition of Nanostructure Materials, Wiley, Weinheim, Germany, 2012.
[11] M. Ritala, M. Leskelä, J.-P. Dekker, C. Mutsaers, P.J. Soininen, J. Skarp, Perfectly conformal TiN and Al_2O_3 films deposited by atomic layer deposition, Chem. Vap. Depos. 5 (1999) 7.
[12] J.W. Elam, S.M. George, Growth of ZnO/Al_2O_3 alloy films using atomic layer deposition techniques, Chem. Mater. 15 (2003) 1020–1028.
[13] R.K. Singh, R. Gandikota, J. Kim, N. Newman, J.M. Rowell, MgB_2 tunnel junctions with native or thermal oxide barriers, Appl. Phys. Lett. 89 (2006) 042512.
[14] G.E. Blonder, M. Tinkham, T.M. Klapwijk, Transition from metallic to tunneling regimes in superconducting microconstrictions: Excess current, charge imbalance, and supercurrent conversion, Phys. Rev. B 25 (1982) 4515.
[15] W.F. Brinkman, R.C. Dynes, J.M. Rowell, Tunneling conductance of asymmetrical barriers, J. Appl. Phys. 41 (1970) 1915.
[16] B.K. Oliver, Ultra-Thin Alumina Barrier Magnetic Tunnel JunctionsPh.D. dissertation Iowa State University, 2003.